Fatigue Characteristics of Graphite/Epoxy Laminates under Compression Loading

M.S. Rosenfeld* and S.L. Huang†
Naval Air Development Center, Warminster, Pa.

A limited number of tests were performed for $R=0$, $-\infty$, and -1 loading to determine the significance of the compression loading and to investigate the failure mechanism. These tests indicated a significant life reduction for both $R=-\infty$ and $R=-1$ loading with respect to tension-tension loading, with the life reduction for $R=-1$ being greater. The mechanism of failure appeared to be local progressive fatigue failure of the matrix near a stress riser, thus causing fiber split, progressive delamination, and resulting fiber buckling, which then precipitates laminate failure.

Nomenclature

R = ratio of mininum to maximum applied cyclic stresses with due regard to sign
T = specimen thickness
w = specimen width
d = hole diameter
σ_{gr} = gross stress = load/$(T\times w)$
σ_{net} = net stress = σ_{gr} − [load/$(T\times d)$] = load/$T(w-d)$

Introduction

THE application of graphite/epoxy laminates to aircraft structures has demonstrated the capability to save weight and improve aircraft performance. The fatigue characteristics of these laminates have been determined for tension-tension loading, and they far exceed the comparable behavior of metals. However, their effect on structural life under compressive and reversed loading is not well characterized. Consequently, it was decided to investigate the compression fatigue characteristics of graphite/epoxy laminates to determine the mechanism of failure and to obtain some preliminary data on the fatigue life characteristics in a laboratory environment. This program was purely exploratory to determine if a more extensive and elaborate program would be required.

Procedure

Test Specimens

The specimens used in the preliminary phase of the program were fabricated from NARMCO 5209 prepreg using MODMOR type II high-strength graphite fibers. The material was laid up in panels using a $[(0, \pm 45\ \text{deg})_S]_3$ balanced layup with the 0-deg fibers on the outside. The stacking sequence was as follows: 0, −45, +45, +45, −45, 0, 0, −45, +45, +45, −45, 0, 0, −45, +45, +45, −45, 0 deg. The panels were cured in an autoclave at 250°F (394 K) and 80 psi (0.55 MN/m^2) and were not postcured. The panels were then cut into 1-in. (25.4-mm) wide specimens, as shown in Fig. 1. Some of the specimens were reinforced with glass-fiber-reinforced plastic (GFRP), as shown in Fig. 1, to provide lateral restraint against bucking.

The second batch of specimens was fabricated from Hercules AS3501-6 prepreg using type A graphite fiber and a balanced $[(0, \pm 45\ \text{deg})_S]_3$ layup. The stacking sequence was the same as for the NARMCO 5209 specimens. The panels were cured at 330°F (439 K) and 80 psi (0.55 MN/m^2). All of these specimens had the GFRP restraint.

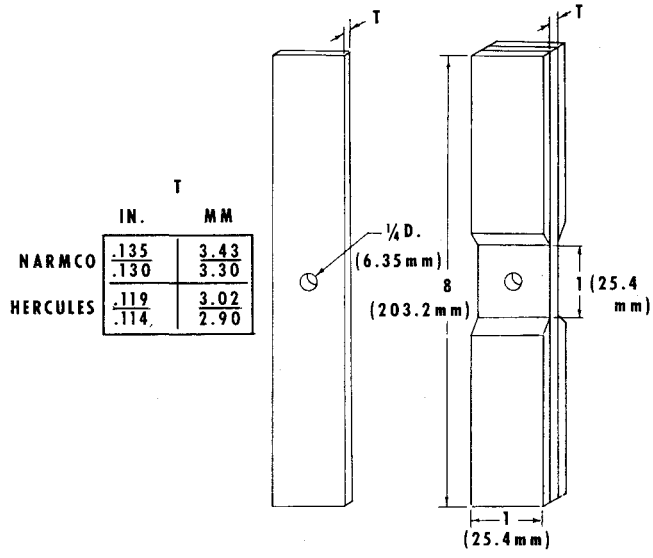

Fig. 1 Test specimen.

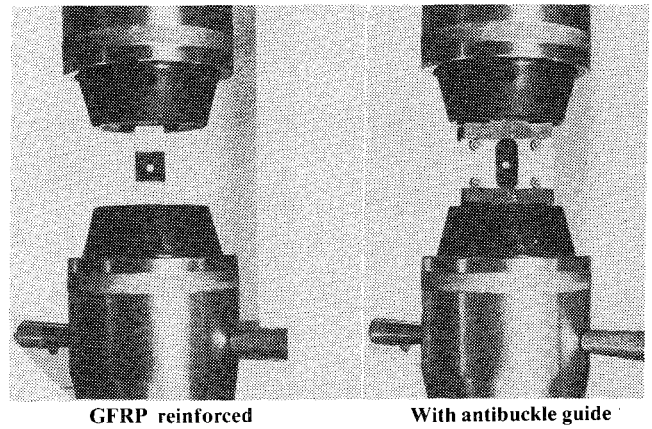

GFRP reinforced With antibuckle guide

Fig. 2 Typical test setup.

Presented as Paper 77-473 at the AIAA Conference on Aircraft Composites: The Energy Methodology for Structural Assurance, San Diego, Calif., March 24-25, 1977; submitted April 7, 1977; revision received Jan. 30, 1978.

Index categories: Structural Materials; Structural Composite Materials; Structural Durability (including Fatigue and Fracture).

*Research Aerospace Engineer, Aero Structures Division, Aircraft and Crew Systems Technology Department.

†Head, Structures R&D Branch, Aero Structures Division, Aircraft and Crew Systems Technology Department.

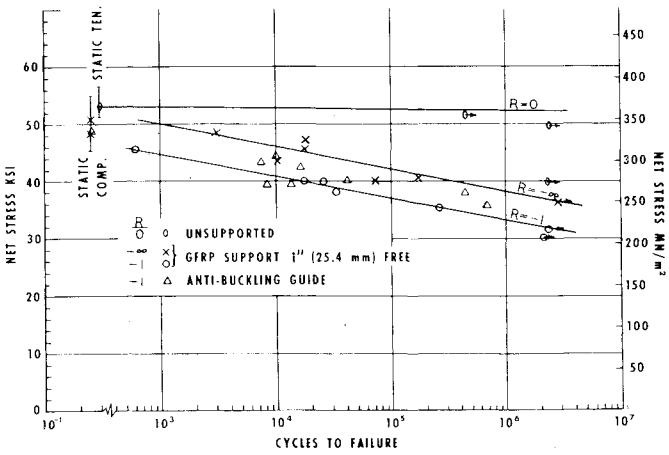

Fig. 3 Life to failure: NARMCO 5209 prepreg.

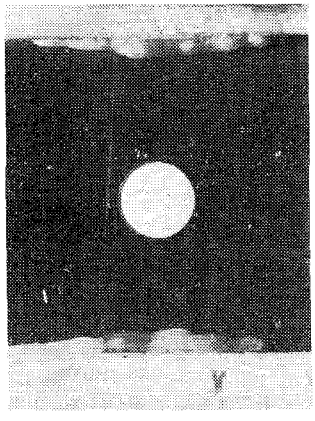

Fig. 4 Typical delamination: 0 deg outer plies.

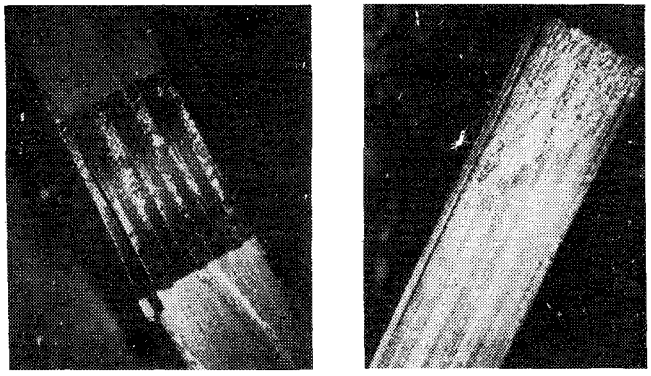

Transverse, NARMCO 5209 Longitudinal, 0-deg outer fibers

Fig. 5 Typical delamination after 5000 cycles at $P = \pm 4000$ lbf.

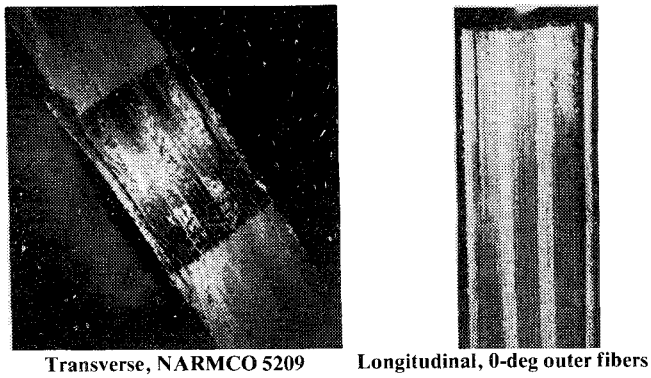

Transverse, NARMCO 5209 Longitudinal, 0-deg outer fibers

Fig. 6 Typical delamination after 7000 cycles at $P = \pm 4000$ lbf.

Subsequent batches of specimens were also fabricated from the Hercules AS3501-6 prepreg. However, these specimens were made with the three outer plies interchanged so that the outer plies were ±45 deg rather than 0 deg to delay delamination. The stacking sequence for these specimens was +45, −45, 0, −45, +45, 0, 0, +45, −45, −45, +45, 0, 0, +45, −45, 0, −45, +45 deg. The last batch of specimens using this layup was made 2 in. (50.8 mm) wide to investigate the effect of specimen width.

Equipment

All tests were performed in an M-T-S closed-loop servohydraulic test machine equipped with "Alignomatic" self-aligning hydraulic grips. The test loads were monitored throughout by an M-T-S amplitude measurement unit and a Hewlett Packard oscilloscope.

Test Procedure

Prior to each test, including the static tests, the test machine grips were aligned using a rigid dummy specimen. Each test specimen was then installed in the grips with a compressive load of approximately 50 lbf (222 N) applied while locking the grip jaws.

Four groups of static tests were performed at the start of the program to establish the method of lateral support to be used for the fatigue tests. These tests were as follows: 1) monotonic tension to failure with no lateral support and 3-in. (76-mm) free length between the grips; 2) monotonic compression to failure with no lateral support and 3-in. (76-mm) free length between the grips; 3) monotonic compression to failure with an aluminum alloy antibuckling guide installed as shown in Fig. 2 [the guide was lined with teflon, was 2¼ in. (5.7 mm) high, and supported the outer ⅛ in. (0.3 mm) on each side of the specimen]; and 4) monotonic compression to failure with GFRP reinforcement at the ends leaving a 1-in. (25-mm) free length, as shown in Fig. 2. The results of these tests are the first four groups in Table 1 and show that the two methods of lateral support were equally effective. Fatigue tests were performed in the same manner as the static tests except that the loading frequency was 5 Hz. Four series of tests were performed initially using the NARMCO 5209 material: 1) no lateral support with 3-in. (75-mm) free length, $R = 0$; 2) GFRP reinforcement with 1-in. (25-mm) free length, $R = -\infty$; 3) GFRP reinforcement with 1-in. (25-mm) free length, $R = -1$; and 4) antibuckling guide restraint with 3-in. (76-mm) length between the grips, $R = -1$.

Since the results of the initial static and fatigue tests with the antibuckling guide and with the GFRP end reinforcement were essentially identical, and since the scatter band for the data obtained with the guide is greater than for the GFRP reinforcement (see Table 1 and Fig. 3), all of the remaining tests were performed using the GFRP reinforced specimen configuration so that the specimens could be readily examined during test.

Results

Static Tests

The static test data are summarized in Table 1. All tension failures occurred through the net section at the hole. All of the compression failures also occurred through the hole; the specimens without the hole failed through the center of the test section where the hole would have been. Although the gross stress at failure for the 2-in. specimens is lower than for the 1-in. specimens for the Hercules material, subsequent work is demonstrating that this is the normal spread for these data.

Constant-Amplitude Fatigue Tests

The lives of the specimens made from NARMCO 5209 prepreg are shown in Fig. 3. The lines for $R = -1$ and $-\infty$ are drawn through the data from the GRFP reinforced specimens; the data from the specimens with the guide are

Table 1 Specimen static strength

	Nominal Width in.	Nominal Width mm	Hole	Outer Ply Angle	Lateral Stabilizer	Failing Load lbf	Failing Load kN	Gross Stress (σ_{gr}) psi	Gross Stress (σ_{gr}) MN/m^2	Net Stress (σ_{net}) psi	Net Stress (σ_{net}) MN/m^2
NMII/NARMCO 5209	1	25.4	yes	0°	None	5250	23.353	38093	262.64	50690	349.50
						5520	24.554	42593	293.67	56714	391.03
						5070	22.552	39030	269.10	51920	357.98
						5280 av.	23.487 av.	39905 av.	275.14 av.	53108 av.	366.17 av.
	1	25.4	yes	0°	None	-3410	-15.168	-24769	-170.78	-32940	-227.11
						-3300	-14.679	-25483	-175.70	-33968	-234.20
						-2990	-13.300	-22852	-157.56	-30380	-209.46
						-3233	-14.381	-24368	-168.01	-32429	-223.59
	1	25.4	yes	0°	Guide	-5420	-24.109	-38560	-265.86	-55015	-379.32
						-4680	-20.818	-34618	-238.68	-46066	-317.62
						-4500	-20.017	-33911	-233.81	-45193	-311.60
						-4867	-21.649	-35696	-246.12	-48758	-336.17
	1	25.4	yes	0°	GFRP	-4800	-21.351	-36185	-249.49	-48255	-332.71
						-5000	-22.241	-38142	-262.98	-50819	-350.39
						-4900	-21.796	-37164	-256.24	-49537	-341.55
	1	25.4	no	0°	GFRP	-8300	-36.920	-62459	-430.64		
						-9170	-40.790	-69004	-475.77		
						-8740	-38.877	-66454	-458.19		
						-8735	-38.855	-65972	-454.86		
HERCULES AS3501-6	1	25.4	yes	0°	GFRP	-5560	-24.732	-46968	-323.83	-62558	-431.32
						-5920	-26.333	-50220	-346.26	-66944	-461.57
						-5740	-25.533	-48594	-335.05	-64751	-446.45
	1	25.4	yes	±45°	GFRP	-5340	-23.754	-45954	-316.84	-61253	-422.33
						-5970	-26.556	-50950	-351.29	-67861	-467.89
						-5655	-25.155	-48452	-334.07	-64557	-445.11
	2	50.8	yes	±45°	GFRP	-9400	-41.813	-41419	-285.58	-47470	-327.30
						-7900	-35.141	-34753	-239.61	-39825	-274.59
						-10400	-46.262	-46212	-318.62	-52953	-365.10
						- 9233 av.	-41.070 av.	-40795 av.	-281.27 av.	-46749 av.	-322.33 av.

Transverse, NARMCO 5209

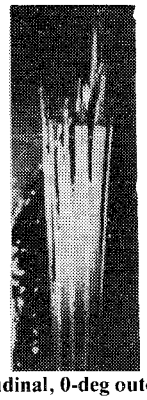

Longitudinal, 0-deg outer fibers

Fig. 7 Typical delamination after failure at $P = \pm 4000$ lbf.

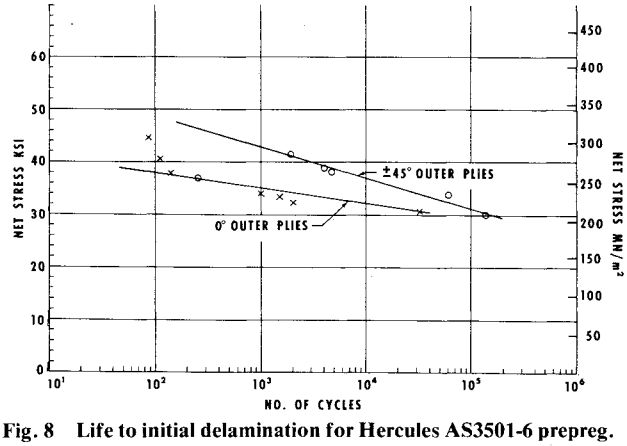

Fig. 8 Life to initial delamination for Hercules AS3501-6 prepreg.

included for information and to show the amount of scatter obtained with the guide. Contrary to our experience with metals, the $R = 0$ condition is not critical; the $R = -\infty$ and -1 conditions, which have large compressive stresses, are the critical conditions. The $R = -1$ loading appears to be more critical than $R = -\infty$. If so, not only compressive stress but also the stress range could be critical in determining the fatigue characteristics of graphite composites.

Both the tensile and compressive loadings caused delamination of the outer plies, as shown in Fig. 4. For the tensile loading, the delamination extended no further than that shown in Fig. 4 and occurred only between the outer 0 deg and the inner plies immediately above and below the hole. For compression loading, the delamination started similar to the tensile loading and then became progressively more severe, as shown in Figs. 5-7; in these figures, the longitudinal cut is through the center of the hole along the 0-deg or loading direction, and the transverse cut is through the center of the hole normal to the loading direction. The life to initial visible delamination is shown in Fig. 8. It is obvious that use of ±45 deg outer plies is considerably more desirable than the 0-deg plies; consequently, all further work was done with the ±45 deg plies on the outside. Figure 9 shows the failure mode of both specimens; there does not appear to be any difference in the extent of delamination between the two. Neither does there appear to be any difference in the failure mode for the 2-in. (50.8-mm) specimens, as shown in Fig. 10.

The life to failure for the 1-in. (25.4-mm)-wide specimens is independent of the outer ply direction (0 or ±45 deg), as shown in Fig. 11; however, based on net section nominal stress, there appears to be a width effect. The same data plotted against gross section stress are shown in Fig. 12; this shows that neither specimen width nor outer ply direction affects the results if gross stress is the parameter.

Variable-Amplitude Fatigue Tests

Tests were performed on a number of GFRP reinforced NARMCO 5209 specimens with 0-deg outer plies to assess the effect of spectrum loading on the fatigue characteristics of the laminate. The MIL-A-8866 fighter spectrum A was used, with the 1-g level flight load as the base and 7.33 g as the limit load

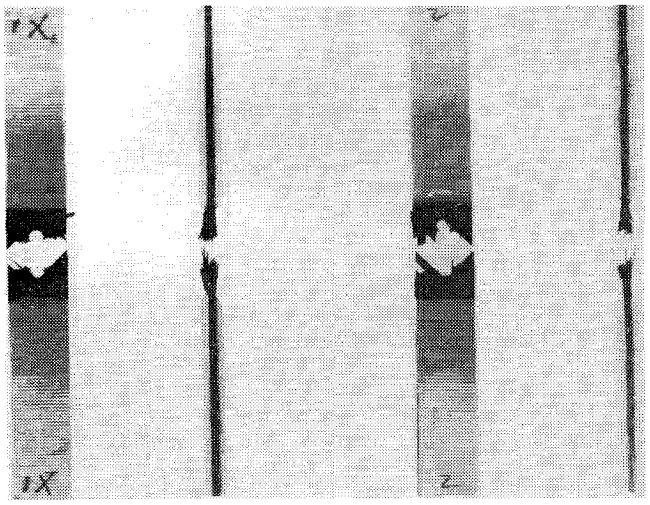

0-deg outer plies ±45-deg outer plies

Fig. 9 Typical failures: 1-in. specimens.

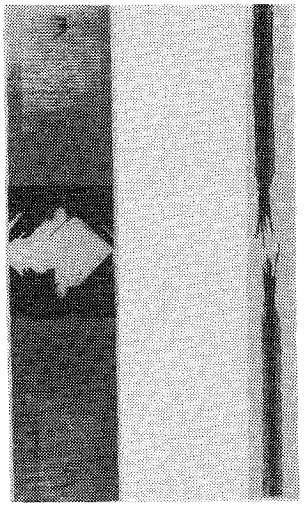

Fig. 10 Typical failure: 2-in. specimen.

±45-deg outer plies.

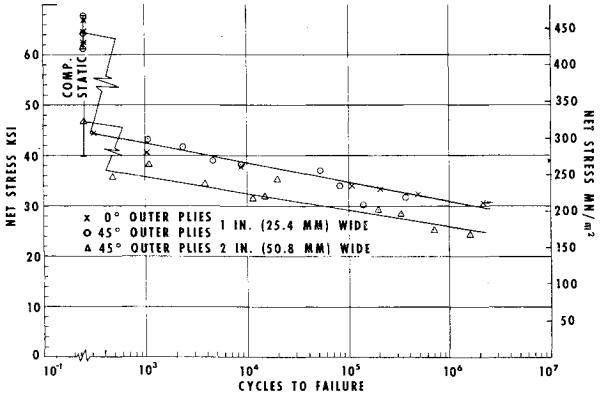

Fig. 11 Life to failure vs net stress: Hercules AS3501-6 prepreg.

Table 2 Sum of damage ratios

Limit stress, ksi	n/N
−32.9	0.006
−31.6	0.113
−29.8	0.042
−28.2	0.173
−27.5	0.447 nf
−27.3	0.066

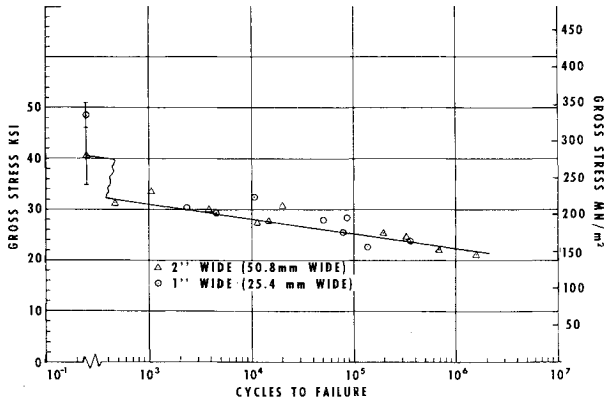

Fig. 12 Life to failure vs gross stress: Hercules AS3501-6 prepreg.

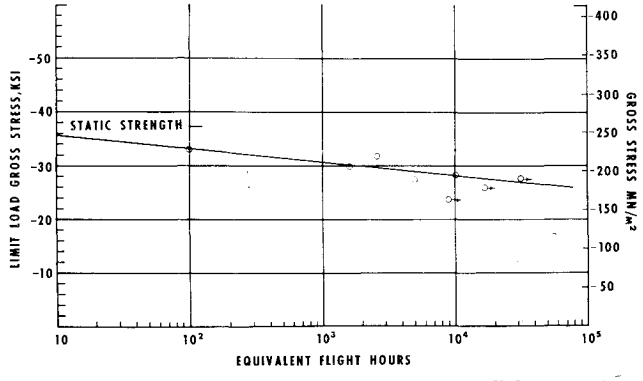

Fig. 13 Life to failure vs limit load gross stress: fighter spectrum, NARMCO 5209 prepreg.

factor. The loading represented that which would be applied to the compression skin during the specified maneuver load frequencies. Tests were conducted to failure or runout for various values of limit load stress. The tests results are shown in Fig. 13. For the current desired factored life of a fighter airplane (12,000 h), the design limit load gross stress in compression should not exceed −28.0 ksi (−193.1 MN/m^2). Although this stress is more than two-thirds of the static strength of this material, it is less than two-thirds of the static strength of the Hercules AS 3501 material, which has the same constant-amplitude fatigue characteristics.

Discussion

The primary objectives of this program were to determine if compressive fatigue loading of graphite/epoxy composite laminates is sufficiently critical to require consideration in structural design and, if so, to determine the failure mechanism involved. The preliminary test results reported herein confirm that compressive fatigue must be a design consideration.

The hypothesized failure mechanism appears to be a local progressive failure of the matrix starting near a stress riser, thus causing fiber split, progressive delamination, and resultant fiber buckling, which then precipitates laminate failure. The first visible indication of failure is delamination between the outermost 0 deg and angle ply laminae regardless of stacking sequence. However, delamination occurs much sooner when the outermost plies are 0 deg than when the outer plies are ±45 deg. This delamination will cause considerable difficulty in service in maintaining a protective paint film on the outer surface; therefore, it is the opinion of the authors that the outer laminae should be angle ply rather than 0 deg.

The delamination progresses as shown in Figs. 5 and 6 until the free sections become critical in column buckling; then the entire section fails, as shown in Fig. 7. This failure hypothesis

is substantiated somewhat by the fact that the lives of the 1-in. (25.4-mm) and 2-in. (50.8-mm)-wide specimens are identical when compared on a gross stress basis, as shown in Fig. 12. This is true only when failure mode is compressive buckling and results from the brittle nature of the material which prevents strain redistribution; this would occur for a ductile material beyond the proportional limit.

It is not known at this time if the matrix failure resulting in delamination results from cycling the interlaminar shear stress, the interlaminar normal stress, or a combination of both. Analytical treatment of this phenomenon and the development of improved matrix materials with better fatigue characteristics should be the subject of further investigation.

The applicability of the Miner cumulative damage rule was applied to the spectrum load test data, with the results given in Table 2. The average damage ratio sum is 0.141, which indicates that the Miner rule is considerably unconservative for compressive loading.

Conclusions

This preliminary program was established for the purpose of determining the significance of compressive loading in fatigue for graphite/epoxy laminates and establishing the failure mechanism under this loading. These limited results lead to the following conclusions:

1) Compressive loads in fatigue produce a significant reduction in fatigue life when compared with the results for tension-tension loading.

2) The mechanism of failure appears to be progressive local fatigue failure of the matrix near a stress riser, thus causing fiber split, progressive delamination, and fiber buckling, which then precipitates laminate failure.

3) The delamination process is delayed by using the outer plies as angle plies rather than 0-deg plies.

4) The Miner cumulative damage rule is unconservative for compressive loading.